Quaternary Research (2017), **88**, 193–205.

doi:10.1017/qua.2017.43

Holocene environmental change inferred from multiple proxies in the mouth of Gomso Bay on the west coast of South Korea

Bing Song[a]*, Sangheon Yi[a]*, Tae-Soo Chang[a], Jin-Cheul Kim[a], Limi Mao[b], Wook-Hyun Nahm[a], Hongjuan Jia[c]

[a]Geologic Environment Division, Korea Institute of Geoscience and Mineral Resources, Daejeon 34132, South Korea
[b]Nanjing Institute of Geology and Palaeontology, Chinese Academy of Sciences, Nanjing 210008, China
[c]Experiment and Practice Teaching Center, Hebei Geo University, Shijiazhuang 05003, China

(Received October 18, 2016; Accepted April 27, 2017)

Abstract

A sediment core (14DH-C01) obtained from the mouth of Gomso Bay, on the west coast of South Korea, was used to obtain high-resolution palynomorph, grain-size, and ^{14}C age data to investigate the Holocene sedimentary environment. The results indicated a transgressive depositional process with four stages controlled by sea-level change, as follows: river-dominated fluvial deposition from the early Holocene to 8.48 cal ka BP; tide-dominated tidal channel fill transgression from 8.48 to 8.08 cal ka BP; tide- to wave-dominated tidal channel fill transgression from 8.08 to 6.98 cal ka BP; and wave-dominated marine transgression from 6.98 cal ka BP to the present. Tidal channel filling was the primary mid-Holocene depositional process, accounting for the high sedimentation rate observed. The different hydrodynamics of the river-dominated, tide-dominated, tide- to wave-dominated, and wave-dominated processes following the changes in sea level may have controlled the transgressive depositional process. This transgressive sedimentary model differs from those of other large river mouth areas (e.g., the Changjiang River) since the mid-Holocene, perhaps resulting from the limited sediment supply in the study area.

Keywords: Holocene; Palynomorph; Sea-level change; Sedimentary environment; Sedimentary model

INTRODUCTION

Estuaries are among the most dynamic geomorphological units in marginal marine environments (Wang et al., 2010). These areas are very sensitive to changes in both sea level and climate (IPCC, 2014), but are also important for human activity. Therefore, there have been several studies of environmental changes during the Holocene in estuarine areas in east Asia (e.g., Wells et al., 1990; Stanley and Warne, 1994; Yi et al., 2003; Tamura et al., 2009; Wang et al., 2011, 2013; Bak, 2015; Feng et al., 2017).

However, most studies have focused on the mouths of very large rivers, such as the Mekong (Tamura et al., 2009), Red (Hori et al., 2004), and Changjiang Rivers (Hori et al., 2001a, 2001b; Wang et al., 2010; Song et al., 2013; Feng et al., 2016). Nearly all of these studies have reported that environmental changes during the Holocene were closely tied to sea-level changes. Coastal progradation was preceded by transgression due to rapid sea-level rise. Sediment deposition in coastal areas generally occurred in the estuarine systems, and a progradational delta deposit gradually covered a transgressive estuarine deposit (Boyd et al., 1992; Tamura et al., 2007). The transition from transgressive estuary to progradational delta occurred from 8.5 to 8.0 cal ka BP (Hori et al., 2002, 2004; Tamura et al., 2009; Song et al., 2013). By contrast, some small estuaries contain retrogradational open-coast tidal flat successions (Kim et al., 1999; Yang et al., 2006; Fan, 2012). Environmental changes in small estuaries during the Holocene have not been well studied. Therefore, using the accessible sedimentary resources, an attempt has been made here to reconstruct the history of paleoenvironmental changes in a small estuary.

Gomso Bay is a relatively small estuary located on the west-central coast of South Korea. Previous monitoring and simulation studies have revealed the transport direction of the surface sediments, as well as the modern processes governing morphological changes in the bay (Wells et al., 1990; Lee et al., 1994, 1999; Yang et al., 2007; Lee, 2010; Choi, 2011; Kang et al., 2014). The sedimentary environment during the Holocene has been reconstructed in previous sedimentological investigations (Chang et al., 1996; Kim et al., 1999; Yang et al., 2006). However, a reliable and chronological history of

*Corresponding authors at: Geologic Environment Division, Korea Institute of Geoscience and Mineral Resources, Daejeon 34132, Korea. E-mail addresses: imbingsong@gmail.com (B. Song); shyi@kigam.re.kr (S. Yi)

changes in the environment during the Holocene in Gomso Bay is lacking due to the limitations of the dating and sediment core drilling techniques of earlier studies. Therefore, to gain a better understanding of the responses to climate change in this area, further studies of paleoenvironmental changes are required.

Utilizing accelerator mass spectrometry (AMS), we present high-resolution ^{14}C age, palynomorph, and grain-size data from a core (14DH-C01) obtained from the mouth of Gomso Bay in 2014 (Fig. 1). We identify the Holocene depositional processes and their responses to sea-level changes in this area. We propose a Holocene evolutionary model to compare Gomso Bay to other large river mouth areas, discussing the diversity of evolutionary mechanisms.

REGIONAL SETTING

Geomorphology and hydrology

The study area is situated at the mouth of Gomso Bay, near Dongho Beach, in the middle of the western coast of South Korea (Fig. 1). It is characterized by a wide tidal flat in the south and a narrow tidal flat in the north. Gomso Bay is controlled by bedrock with a funnel-shaped morphology. It is 5–8 km wide at the mouth and 20 km long from head to mouth. The sediments of Gomso Bay primarily originate from the Chujin and Kangsun channels (Yang et al., 2007; Choi et al., 2013), but there is little sediment supply from the major rivers. From east to west, the bay is divided into inner, middle, and outer regions (Yang et al., 2007). The grain size gradually coarsens and the slope gradient gradually steepens seaward (Lee et al., 1994; Yang et al., 2007). In addition, more than 80% of the estuary is occupied by extensive intertidal flats, which are best developed in the south (Yang et al., 2007). Sandbars are common in the lower intertidal flats, and tidal creeks are present in the middle and upper flats (KORDI, 2007; Lee, 2010).

The study area is characterized by a macrotidal regime with a spring and neap tidal range of 6.0 and 3.5 m, respectively (Yang et al., 2006; NORI, 2007). The ebb and flood current speeds of the Gomso tidal channel are 1.15 and 1.50 m/s, respectively (NGII, 1981; Choi, 2011). The area is also affected by the Asian Monsoon. In the summer, weak southerly winds maintain calm seas and low wave energy, but much higher wave energy is produced by strong northerly winds during the winter (Yang et al., 2006). In addition, waves can be over 2 m high during storm periods (Choi et al., 2013).

Climate and vegetation

The annual precipitation is primarily controlled by the summer monsoon climate, with 70% of precipitation occurring during the summer rainy season (Choi et al., 2013). The annual average precipitation can reach 1100–1300 mm (KMA, 1998). The modern vegetation in the Bay is characterized by a mixed

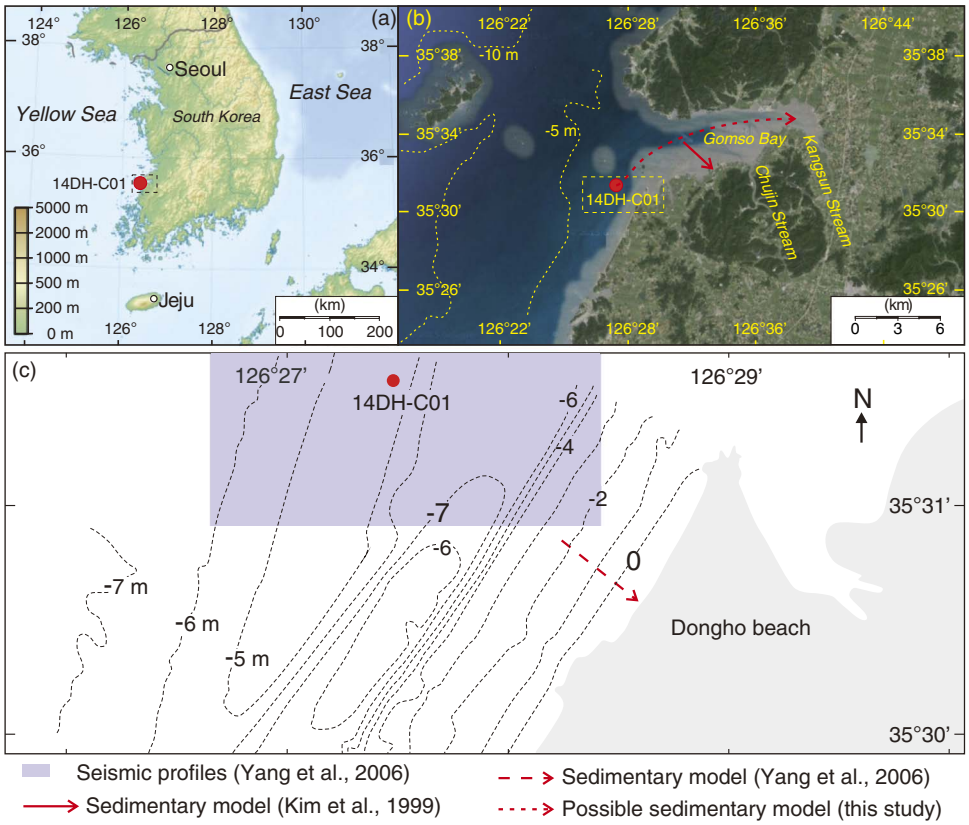

Figure 1. (color online) (a) Geomorphologic map of South Korea (modified from https://upload. wikimedia.org/wikipedia/commons/a/a8/Korea_topographic_map.png). (b) The mouth of Gomso Bay (modified from Google maps). (c) Location of the drill core. The seismic profiles are taken from Yang et al. (2006). The dashed lines in Figure 1a and c are depth contours.

https://doi.org/10.1017/qua.2017.43 Published online by Cambridge University Press

forest of pine and oak trees, dominated by *Pinus densiflora*, *Pinus thunbergii*, *Quercus variabilis*, *Quercus mongolica*, *Quercus serrata*, *Quercus dentata*, *Quercus acutissima*, and *Carpinus turczaninovii*, and artificially planted *Pinus rigida*, *Cryptomeria japonica*, and *Chamaecyparis obtusa* var. *foraurea*. Halophytes are present in the salt marshes, including *Angelica utilis*, *Salicornia herbacea*, *Suaeda japonica*, and *Phragmites communis*. Naturalized herbs include *Rumex crispus*, *Panicum dichotomiflorum*, and *Aster pilosus*, which tend to grow on the border between the land and the coast (Oh and Rho, 2013).

MATERIALS AND METHODS

The 14DH-C01 core was sampled from latitude/longitude 35°31.614'N, 126°27.52'E at a water depth of 4.3 m. In this study, we focused on the upper 22 m of the core. The core was split, photographed, and divided into 124 subsamples at the Korea Institute of Geoscience and Mineral Resources (KIGAM) for pollen, dinocyst, and grain size analyses. Palynomorph samples weighing about 11–14 g after drying were examined using an equal-volume sampling method.

Pretreatment and identification of micropaleontological samples were performed at KIGAM. Samples were prepared following the procedures outlined by Faegri and Iyersen (1989). Dried samples were obtained from KIGAM, weighed, and then exotic *Lycopodium* spores were added to measure the palynomorph relative abundances. The samples were treated with dilute 15% hydrochloric acid (HCl) to remove carbonates, 45% hydrofluoric acid to dissolve siliceous materials, and 15% sodium hydroxide to deflocculate the matrix and prepare the palynomorph spectra. Then HCl was again used to remove carbonates, and samples were sieved through a 10 µm mesh. Pollen, spores, and dinocysts were examined using a Nikon microscope at 400× magnification; however, a 620× magnification was used if identification was difficult. In general, more than 200 palynomorph grains or two slides were counted for every sample. However, the number of palynomorph grains in several sandy samples was very low (less than 80), so we discarded the data. Ultimately, 41 samples were included in the study. The palynomorph counts of 28 samples were in the range of 200–456 grains, and the remaining 13 samples were in the range of 80–199 grains. We obtained modern and fossil pollen information from the State Key Laboratory of Palaeobiology and Stratigraphy at the Nanjing Institute of Geology and Palaeontology, Chinese Academy of Sciences; the Quaternary Geology Research Department, Geological Research Division, Korea Institute of Geoscience and Mineral Resources; and reference plates from Academia Sinica (1976, 1979).

We selected 10 samples (9 shell samples and 1 plant fragment sample) for AMS ^{14}C dating (Table 1). Based on a Libby half-life of 5,568 years, we used OxCal v4.2.4 (http://c14.arch.ox.ac.uk; Bronk Ramsey and Lee, 2013) and conventional radiocarbon age data set of Reimer et al. (2013) to calibrate the ages.

For the evaluation of grain size, dry samples of about 300 mg were treated with 35% hydrogen peroxide to decompose organic matter and then boiled in 1N HCl for 1 h to remove carbonates and iron oxides. After rinsing with distilled water, the samples were treated with an ultrasonic vibrator for 15 min to maintain suspension and to facilitate dispersion. A Microtrac 2000 laser analyzer automatically provided the percentages of clay, silt, and sand in the subsamples.

RESULTS

Chronological control and sedimentation rate

We obtained 10 AMS radiocarbon ages from the 14DH-C01 core (Table 1), and then used these to determine the chronology of the palynomorph spectrum at the mouth of Gomso Bay. From the age and depth data, we constructed the age frame using Clam 2.2 (Fig. 2; Blaauw, 2010). We also used Bacon 2.2 (Blaauw and Christern, 2011, 2013) to build the age frame, which is described in the supplementary material.

Table 1. Summary of radiocarbon ages obtained from core 14DH-C01.

Lab No. KGM-	Sample No.	Core depth (m)	Material	Radiocarbon age (^{14}C yr BP)	δ^{13}C (‰)	Calibrated ^{14}C age (cal yr BP)
Ica150007	DH01-6	5.34	Shell	5750 ± 40	3.9	6180 ± 56
Ica150008	DH01-7	6.07	Shell	5900 ± 40	–1.7	6316 ± 43
Ica150010	DH01-9	9.13	Shell	6500 ± 40	0.7	7007 ± 68
Iwd150089	DH01-11	10.63	Plant fragment	7370 ± 40	–30.1	7994 ± 39
Ica150012	DH01-14	13.8	Shell	7740 ± 40	0.2	8217 ± 53
Ica150013	DH01-15	14.08	Shell	7690 ± 40	–0.3	8145 ± 60
Ica150014	DH01-17	17.2	Shell	7670 ± 40	0.9	8119 ± 57
Ica150015	DH01-18	17.55	Shell	7940 ± 40	–1.4	8394 ± 41
Ica150016	DH01-21	18.88	Shell	8030 ± 40	1.1	8480 ± 50
Ica150017	DH01-22	19.53	Shell	8050 ± 50	–1.5	8499 ± 60

Note: ^{13}C/^{12}C and conventional ^{14}C were measured by accelerator mass spectrometer (AMS) in KIGAM. Calibrated ^{14}C ages were calculated using OxCal OxCal OxCal v4.2.4 software (Ramsey, (2013). If the sample wais shell, the chosen parameters was choice thatwere the marine curve (Reimer et al., 2013) and local marine delta R (-111, 45; Kong and Lee, 2005). If the sample wais a plant fragment, the chosen parameter was choice that the IntCal13 atmospheric curve (Reimer et al., 2013).

https://doi.org/10.1017/qua.2017.43 Published online by Cambridge University Press

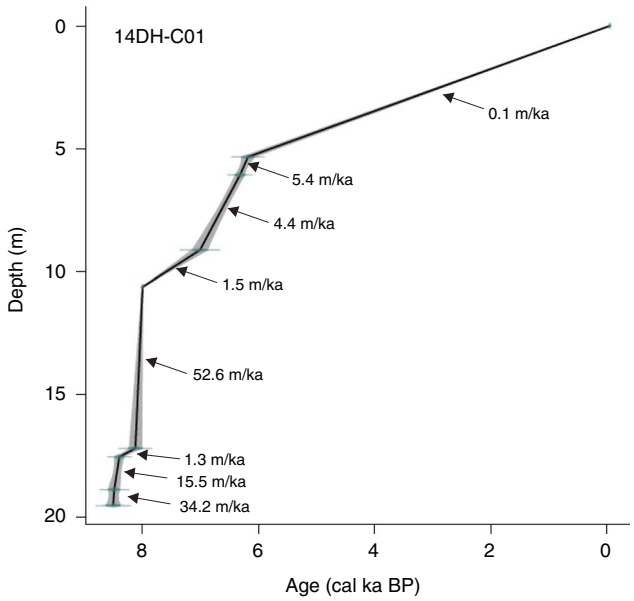

Figure 2. (color online) Age–depth curve and sedimentation rates of core 14DH-C01. The age frame was constructed using Clam 2.2 (Blaauw, 2010).

We did not consider sediment compaction effects or basin subsidence. In addition, two ages obtained from a depth of 13.8 m and 14.08 m were older than the age of the sample in the lower part. These ages may indicate reworking, so we excluded them from the Clam model.

The sedimentation rate gradually decreased from 34.2 to 1.3 m/ka from 8499 to 8119 cal yr BP, and gradually increased from 1.5 to 5.4 m/ka from 7994 to 6180 cal yr BP (Fig. 2).

Sedimentary characteristics

Based on the sediment composition, grain size, texture, and faunal content, the Holocene sediments were divided into four units in ascending order: U1, U2, U3, and U4 (Figs. 3 and 4).

U1 (22.0–19.0 m)

The unit consisted of yellowish-brown coarse sand with subangular gravel or pebbles (Figs. 3 and 4a) and some semi-consolidated homogeneous yellowish-brown clayey sand with rare laminae. The data indicated an age of 8499 cal yr BP at a depth of 19.53 m for this section (Table 1).

U2 (19.0–15.0 m)

The unit consisted of dark yellow, very fine sandy silt with upward fining (Figs. 3 and 4b). The mud content ranged from 15% to 70%, and the mean grain size ranged from 5 to 3 phi. Several mud–sand couplets about 0.2–1 cm thick were observed. The mud layer consisted of silty clay. The sand layer consisted of fine to coarse sand. Shell fragments were scattered throughout this unit, including some thin layers about 1–3 cm thick.

U3 (15.0–9.0 m)

The unit consisted of dark yellow, very fine sandy silt to grayish-yellow, fine- to medium-grained sand with upward coarsening (Figs. 3 and 4c). There were several mud-sand couplets, with the thickness of sand layer increasing gradually. Some small shell fragments were scattered throughout the unit. There was a 13-cm-thick shell layer in the upper section, which was in contact with the upper unit, U4. The mud content and mean grain size changed from 70 to 0% and 4.5 to 2 phi, respectively.

U4 (9.0–0 m)

The unit mainly consisted of grayish-yellow, very fine- to medium-grained sand with a few weak sand-mud couplets (Figs. 3 and 4d). The thickness of the mud layer was about 0.2–1 cm and showed slight disturbance in some sections (Fig. 4e). There were some cross-laminations and some shell fragments throughout this unit. The mud content and mean grain size were about 0–30% and 4–2 phi, respectively. There were two age estimations for this unit: 6180 and 6316 cal yr BP.

Palynomorphs and palynomorph spectrum

Pollen, fern spores, freshwater algae, microforaminiferal linings, and dinocysts were identified. We divided these into six groups according to their relationship with the parent plants and biotope as follows: arboreal pollen (AP), non-arboreal pollen (NAP), fern spores, freshwater algae, microforaminiferal linings, and dinocysts (Fig. 5). Only the principal palynomorphs are included in the diagrams. The term palynomorph is used for all counted pollen, spores, and other grains, whereas the term pollen refers only to pollen grains (Li et al., 2006).

In the lower sedimentary unit (22.0–19.0 m depth) of the 14DH-C01 core, the sediments consisted of gravel and coarse sand. We did not perform pollen analyses due to their relatively low abundances. In the upper part (9.5–0 m depth), the sediments consisted of very fine- to medium-grained sand, yielding palynomorph data of low abundances. For some sections, such as 10.5–9.8 m depth, there were no sediment samples (Figs. 5 and 6). We divided the palynomorph spectrum into two zones, zone I and zone II, based on the results of CONISS analysis (Fig. 5; Grimm, 1991, 1992).

Palynomorph zone I (19.0–5.0 m)

In zone I, the relative abundances of AP, NAP, and dinocysts were about 32.1, 29.0, and 30.7%, respectively. AP was dominated by *Quercus* (deciduous), *Quercus* (evergreen), and *Pinus*. The dominant components of the NAP were Gramineae, Cyperaceae, *Potamogeton*, Chenopodiaceae, and *Artemisia*. Dinocysts consisted of *Operculodinium centrocarpum* and *Spiniferites bulloides*. The number of freshwater algae and spores was relatively low, with average relative abundances of less than 0.5%. The main components

https://doi.org/10.1017/qua.2017.43 Published online by Cambridge University Press

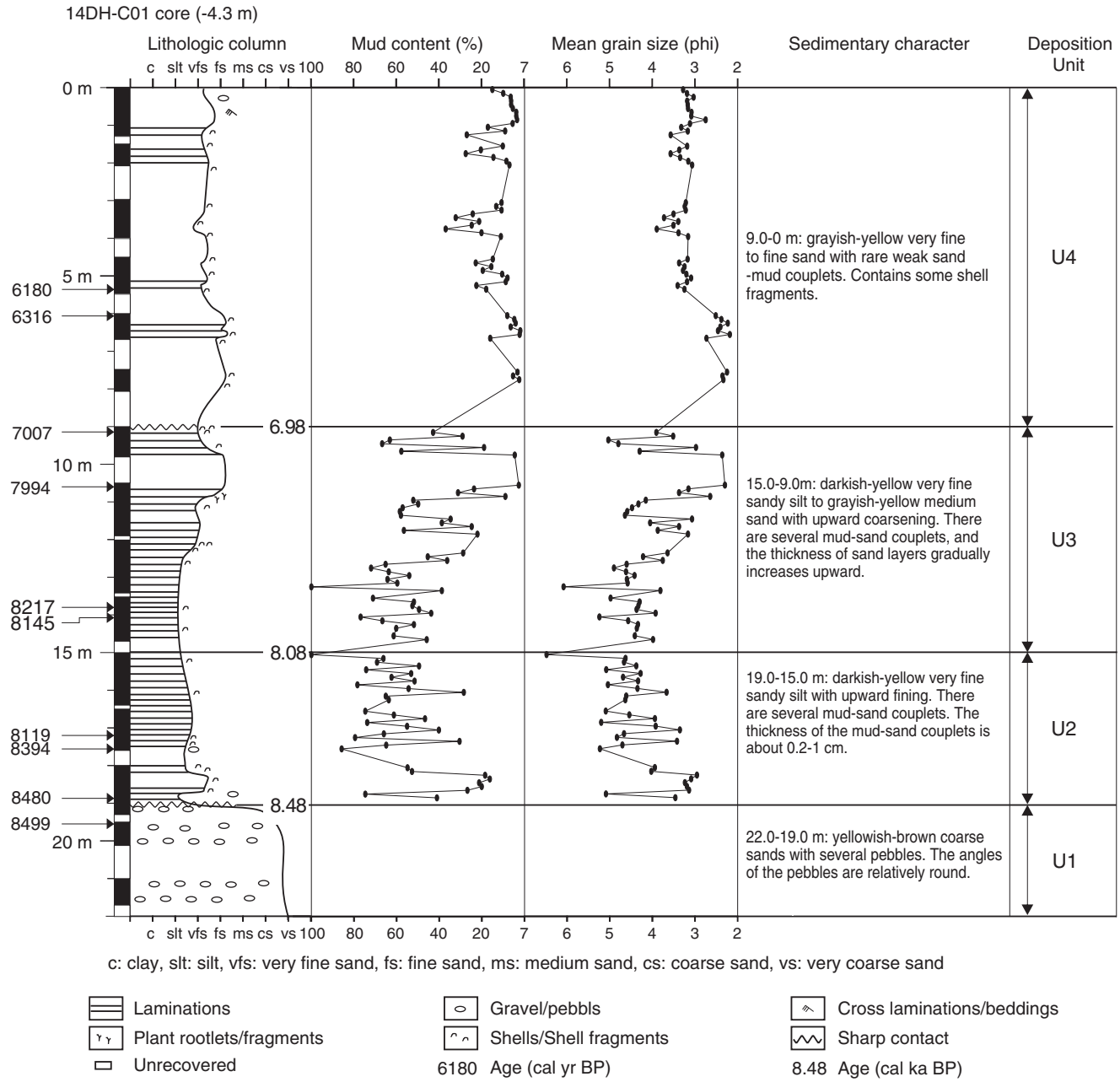

Figure 3. Lithological column and sedimentary units of core 14DH-C01. Age is the median of the calibrated age.

of freshwater algae were Pediastraceae and *Concentricystes*. Polypodiaceae, *Pteridium*, and Gleicheniaceae were the dominant fern components.

This palynomorph zone can be divided into two subzones, Ia and Ib, with the boundary between them occurring at a depth of about 14.7 m. Zone Ia contained AP, dominated by *Pinus*, *Quercus* (deciduous), and *Quercus* (evergreen), with average relative abundances of about 3.9%, 5.4%, and 12.3%, respectively. These relative abundances were slightly lower than those in Ib (about 4.3%, 6.3%, and 17.1%, respectively). In zone Ia, the dominant NAP components were Gramineae, Cyperaceae, *Potamogeton*, Chenopodiaceae, and *Artemisia*, with average relative abundances of about 3.8%, 9.9%, 6.4%, 8.7%, and 1.7%, respectively. These average relative abundances were slightly higher than those in Ib (about 2.6%, 8.4%, 5.8%, 7.7%, and 1.1%, respectively). In zone Ia, the average relative abundances of the dinocysts *Operculodinium centrocarpum* and *Spiniferites bulloides* were 3.1% and 20.7%, respectively; in zone Ib, they were about 5.2% and 22%, respectively.

Palynomorph zone II (5.0–0 m)

Only three samples were available from zone II. The average relative abundance of AP was 37.2%. *Pinus*, *Quercus* (evergreen), and *Quercus* (deciduous) were the main components,

https://doi.org/10.1017/qua.2017.43 Published online by Cambridge University Press

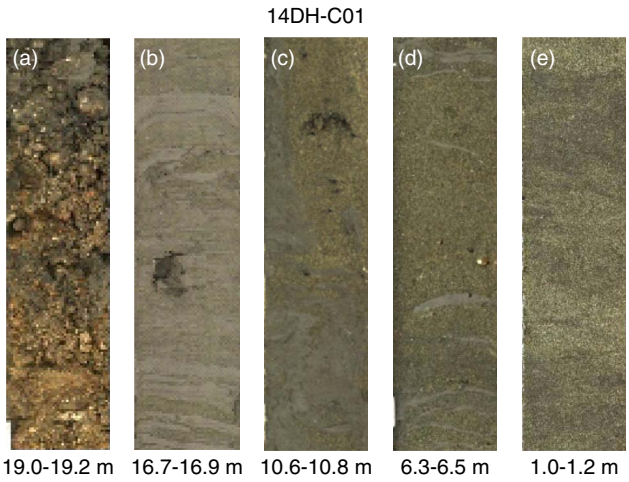

Figure 4. (color online) Major sedimentary structures in core 14DH-C01. (a) Yellowish brown, coarse sand with subangular gravel or pebbles. (b) dark yellow, very fine sandy silt with thin mud–sand couplets. (c) grayish-yellow, fine sand with disturbed thin mud–sand couplets. (d) grayish-yellow, fine- to medium-grained sand with thin mud layers. (e) grayish-yellow, very fine sand with weak mud–sand couplets. Scale bar = 0.1 m.

with relative abundances of about 20.4%, 5.8%, and 6.9%, respectively. The relative abundance of NAP was 25.7%, consisting of Gramineae, Cyperaceae, *Potamogeton*, and Chenopodiaceae. *Operculodinium centrocarpum* and *Spiniferites bulloides* were the main dinocyst components, with an average relative abundance of about 32.5%. However, the average relative abundances of *Operculodinium centrocarpum* and *Spiniferites bulloides* were about 17.8% and 14.1%, respectively.

DISCUSSION

Palynomorph provenance and environmental proxies

Gomso Bay is a small estuary with two small streams, partially surrounded by hills (Fig. 1). In the study area, the dinocysts and microforaminiferal linings came from a marine environment, making them ideal environmental proxies for salt water. The terrigenous materials of pollen, ferns, spores, and freshwater algae primarily came from the local area. In addition, the primary AP in the upper part of the core consisted of *Pinus* and *Quercus*, similar to the modern vegetation in the region. The palynological spectrum of the sediment core of 14DH-C01 could reveal past vegetation and climate changes. However, the sedimentary environment was unstable (Fig. 3), affecting the spectrum of pollen, ferns, spores, and freshwater algae in the sediment. Therefore, in this study, we used only the pollen of the herb Chenopodiaceae as a proxy for the coastal environment (Byeong-O et al., 2006; Jun et al., 2010).

Interpretation of sedimentary units and depositional processes

The sediments of U1 (22.0–19.0 m, early Holocene–8.48 cal ka BP; Fig. 6) consisted of yellowish-brown coarse

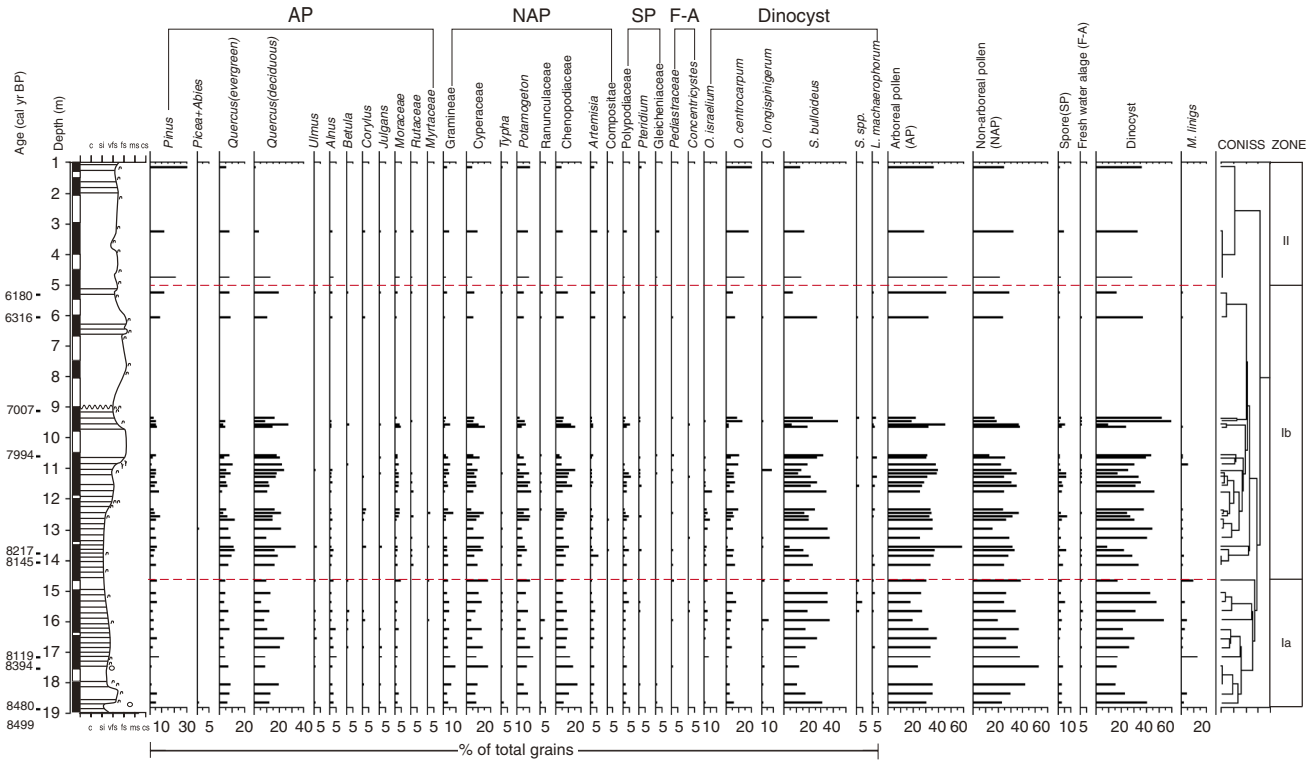

Figure 5. (color online) Palynomorph spectrum of core 14DH-C01 showing the palynomorph zones.

https://doi.org/10.1017/qua.2017.43 Published online by Cambridge University Press

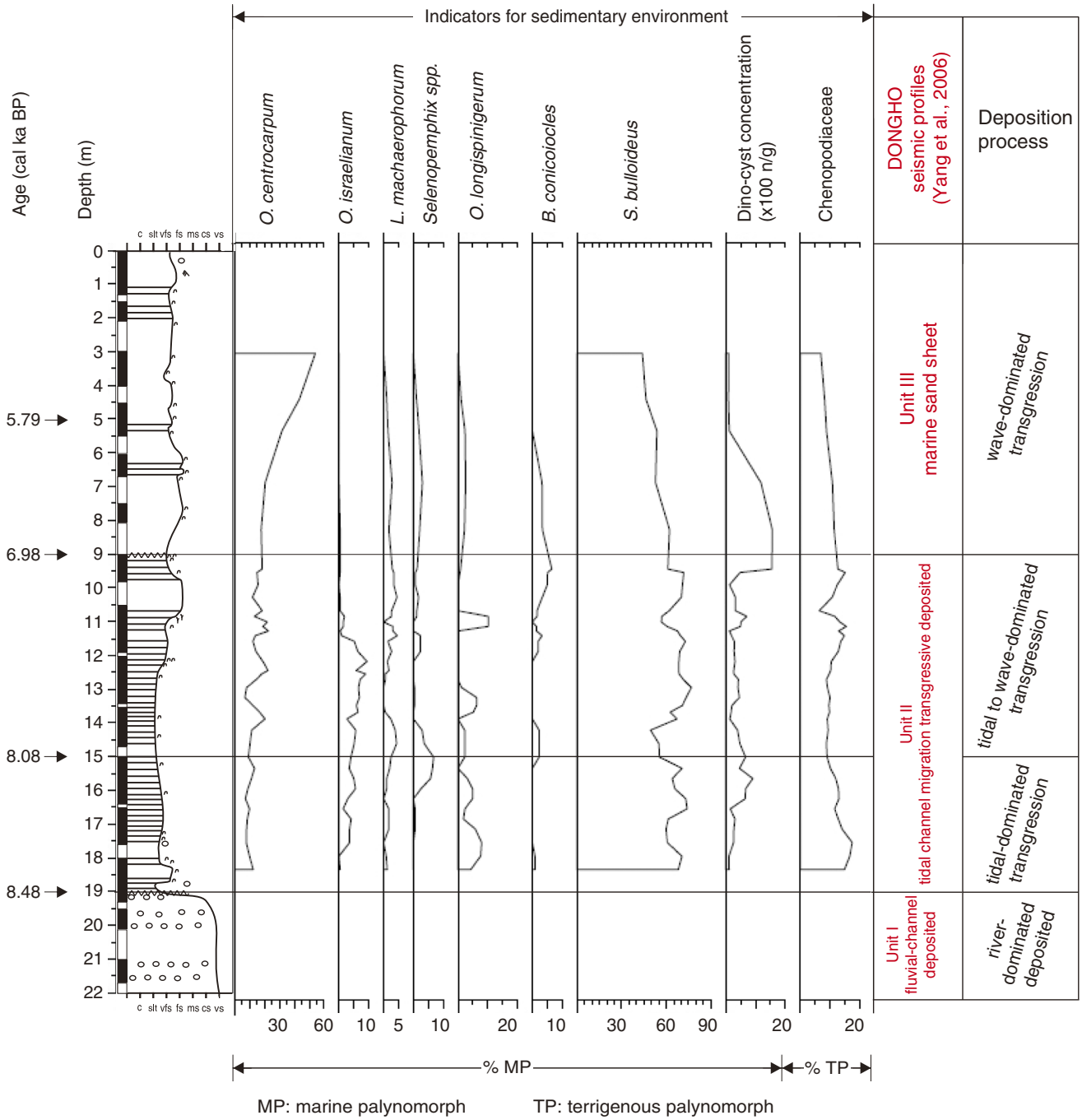

Figure 6. (color online) A composite diagram showing changes in depositional processes. The palynomorph curve is based on a three-point running average. The DONGHO seismic profiles are taken from Yang et al. (2006).

sand with subangular gravel or pebbles (Figs. 3 and 4a), consistent with those described by Yang et al. (2006). Primary sediment deposition occurred earlier than 8.48 cal ka BP and was rarely affected by the ocean dynamics. This unit was previously interpreted as a river-dominated fluvial channel (Yang et al., 2006).

The mud-sand couplets of U2 (19.0–15.0 m, 8.48–8.08 cal ka BP; Fig. 6) suggest tidal effects (Hori et al., 2001a). High relative abundances of *Operculodinium israelianum* in nearshore sites, in which high upper-water salinities prevail (Zonneveld et al., 2013), along with a gradual increase in the abundance of marine palynomorphs, suggest a gradually increasing marine influence (Fig. 6; Shin et al., 2007, 2010, 2013; Zonneveld et al., 2013). The upward decrease in the relative abundance of Chenopodiaceae among the terrestrial palynomorphs also suggests that this unit represents a transgressive depositional system (Fig. 6; Jun et al., 2010). The unit is similar to the lower section of the small-scale cut-and-fill pattern of tidal channel migration in a transgressive depositional environment described by Yang et al. (2006) (Fig. 6), representing a tide-dominated tidal channel fill environment (Yang et al., 2006).

https://doi.org/10.1017/qua.2017.43 Published online by Cambridge University Press

The mud–sand couplets of U3 (15.0–9.0 m, 8.08–6.98 cal yr BP; Fig. 6) also suggest tidal effects (Hori et al., 2001a). Abundances of dinocysts, such as *Operculodinium centrocarpum*, *Operculodinium israelianum*, *Spiniferites bentori*, and *Spiniferites bulloideus*, suggest a strong marine influence. In this unit, the mud-sand couplets gradually thicken upward and grain size gradually coarsens (Figs. 3 and 4c), indicating the influence of gradually strengthening hydrodynamics. The shell layer and sharp contact separating units, U3 and U4, were interpreted as a wave ravinement surface, which formed during the retreat of the sandbar (Yang et al., 2006). This indicates that the environment gradually transitioned from tide-dominated to wave-dominated transgressive deposition, similar to the scenario described for the upper part of a transgressive deposit in which the small-scale cut-and-fill pattern resulted from tidal channel migration (Yang et al., 2006).

U4 (9.0–0 m, 6.98 cal ka BP–present) contained some sand–mud couplets with a very thin mud layer and several other layers, indicating very strong hydrodynamics (Coleman and Wright, 1975). *Operculodinium centrocarpum* is a cosmopolitan species (Zonneveld et al., 2013); however, the relative abundance of *Spiniferites bulloides* gradually decreased from the central Yellow Sea to coastal areas (Shin et al., 2007, 2013). The relative abundance of *Operculodinium centrocarpum* increased gradually, while that of *Lingulodinium machaerophorum*, *Spiniferites bulloides*, *Selenopemphix* spp., as well as of dinocysts decreased (Fig. 6). These observations suggest a possible decrease in salt-water influence (Shin et al., 2007, 2010, 2013; Zonneveld et al., 2013). The sediments primarily consist of sands, and the present-day landform is a sandbar that formed from wave-dominated transgressive deposits (Yang et al., 2006). This is similar to the marine sand sheet formation derived from reworking of the shoreline during the transgression as described by Yang et al. (2006).

Paleoenvironmental changes and responses to sea-level changes

The evolution of the sedimentary environment during the Holocene is closely associated with sea-level changes at the mouths of estuaries (Stanley and Warne, 1994). Along the northwestern Pacific coast, sea level rose rapidly during the early Holocene to 8.0 cal ka BP, after which the rate of sea-level rise was relatively slow (Chen and Stanley, 1998; Kim et al., 1999; Chough et al., 2000; Chang and Choi, 2001; Zong, 2004; Chen et al., 2008; Song et al., 2013; Wang et al., 2013). However, reports of sea-level rise after 6.0 cal ka BP have differed (Fig. 7). Some researchers suggest that the sea level continued to rise up to the present (Kim et al., 1999; Chough et al., 2000; Zong, 2004), whereas others suggest that it was higher during mid-Holocene than at present (Munyikwa et al., 2008; Song et al., 2013; Nahm and Hong, 2014; Bak, 2015; Park et al., 2015). Nonetheless, overall the sea level was relatively stable after approximately 6.0 cal ka BP.

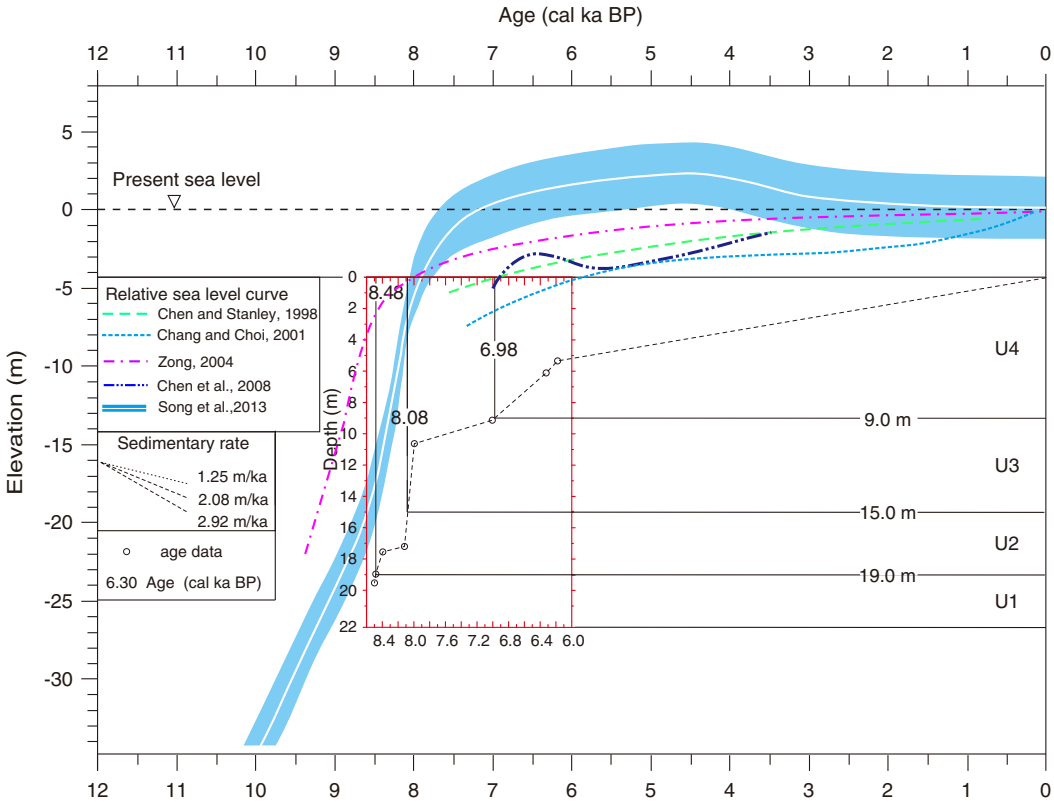

Figure 7. (color online) Sediment accumulation curve and sedimentary processes of core 14DH-C01, with the relative sea-level curve for a nearby area (Chen and Stanley, 1998; Chang and Choi, 2001; Zong, 2004; Chen et al., 2008; Song et al., 2013).

https://doi.org/10.1017/qua.2017.43 Published online by Cambridge University Press

During early Holocene to ~8.08 cal ka BP, the sea level in the study area rose rapidly, and river-dominated fluvial channel deposition was followed by tide-dominated tidal channel fill retrogradation (Dalrymple et al., 1992; Boyd et al., 2006; Kim et al., 2006). During this retrogradation process, the rivers may have had a weak influence, while the marine environment may have had a strong influence. Following the rapid rise in sea level and landward coastal movement, the relative abundances of *Operculodinium israelianum*, *Lingulodinium machaerophorum*, *Selenopemphix* spp., and dinocysts gradually increased, whereas the relative abundance of Chenopodiaceae decreased. In addition, the sedimentation rate decreased gradually from 34.2 to 1.3 m/ka during 8.48–8.12 cal ka BP (Figs. 2 and 7) but decreased rapidly during 8.48–8.12 cal ka BP, possibly due to the rapid rise in sea level in the Yangtze Delta area (Song et al., 2013; Wang et al., 2013) (Fig. 7). The decreasing sedimentation rate, grain size, and thinning of the mud-sand couplets indicate that the study area gradually became a tidal channel with tidal fill deposition. The mid-Holocene sedimentation rate was relatively high in the study area, perhaps because of a transgressive deposition mode of tidal channel migration (Kim et al., 2006).

During 8.08–6.98 cal ka BP, the sedimentary environment represented a tide- to wave-dominated tidal channel fill transgression (Fig. 7). The hydrodynamics were gradually strengthening in the study area, and the grain size of the sediments began to coarsen (Fig. 6), followed by a continued rise in sea level. The sedimentation rate gradually increased from 1.5 to 5.4 m/ka during 7.99–6.18 cal ka BP (Figs. 2 and 7). However, after 6.98 cal ka BP, the sea level was relatively stable or decreased only slightly, and the area experienced wave-dominated transgression. Increased amounts of fresh water transportation from the estuary reduced the influence of salt water in the marine palynomorphs.

Holocene sedimentary model and sedimentary process

Several previous studies have described sedimentary models for Gomso Bay and the adjacent area (Kim et al., 1999; Chang and Choi, 2001; Yang et al., 2006; Fan, 2012). However, sediment cores with high-resolution grain size and dating analyses are still lacking from the study area. Therefore, it is still necessary to develop a Holocene sedimentary model with isochrons.

Holocene sedimentary model

Kim et al. (1999) suggested the presence of transgressive Holocene units in the extensive Gomso Bay tidal flat (Fig. 8b). The Holocene stratigraphy unconformably overlies the weathered Cretaceous volcanic rocks (Kim et al., 1999) and may be divided into five depositional units. In ascending order, these facies include salt marsh flat, mud flat, mixed flat, sand flat, and subtidal flat. The retrograde stratigraphy consists of an upward coarsening late Holocene succession (Kim et al., 1999; Fan, 2012).

In contrast, Yang et al. (2006) described a scenario of transgressive sedimentation and stratigraphic evolution of a wave-dominated macrotidal coast (Fig. 8c), dividing the stratigraphy into three units, in ascending order, as follows: tidal flat deposits, transgressive marine sand, and barrier island deposits. In addition, a wave ravinement surface was observed between the tidal flat deposits and the transgressive marine sand sheet (Yang et al., 2006).

Based on the data collected from different study areas, several scenarios could evolve (Fig. 1). Whereas Kim et al. (1999) based their study on Gomso Bay, Yang et al. (1999) focused on adjacent offshore and onshore areas. Lack of high-resolution data could be another possible explanation. Nonetheless, there was still considerable agreement among the studies. The tidal flat deposits of Yang et al. (2006) are similar to Kim et al.'s (1999) sequence of salt marsh, mudflat, and mixed-flat deposits, and the transgressive marine sand is similar to the sand flats described by Kim et al. (1999; Fig. 8c).

Previous studies have focused on tidal flats or coastal areas, discussing sedimentary models based on the sedimentary stratigraphy that followed the evolution of the flats or coast (e.g., Kim et al., 1999; Yang et al., 2006; Fig. 1b and c). In this study, we found paleo-fluvial deposits below the tidal channel fill (Fig. 8a). We traced the likely direction of paleo-fluvial flow and combined the results of Kim et al. (1999) and Yang et al. (2006) to develop a Holocene sedimentary model for Gomso Bay (Fig. 8d).

The changes in the sedimentary environment during the Holocene were likely determined primarily by changes in sea level and the accompanying hydrodynamics (Fig. 8d). The different hydrodynamics of river-dominated, tide-dominated, tide- to wave-dominated, and wave-dominated processes during the different periods following changes in the sea level controlled the transgressive deposition.

Previous studies have shown that the deposited sediment was sequentially controlled by tide-dominated, mixed-energy (tide- to wave-dominated), and wave-dominated depositional processes from the inner bay to the mouth of Gomso Bay (Yang et al., 2007); the landward area of Gomso Bay still contains the Kangsun River. The sedimentary facies produced by the progression of tide-dominated deposition to wave-dominated transgression are similar to the mud flats and mixed flats described in previous studies (Kim et al., 1999; Yang et al., 2006; Fan, 2012), and the wave-dominated marine sand sheet is similar to the previously described sand flats and subtidal flats (Kim et al., 1999; Fan, 2012).

Sedimentary process during the Holocene

Lack of high-resolution data makes determining the origins and depositional stages of Holocene sediments difficult in the study area. Recent studies have shown that the surface grain size gradually coarsens from the inner bay to the mouth of Gomso Bay, and that the finer grains are transported from the fluvial and inner areas of the bay to the middle and outer areas (Lee, 2010; Kang et al., 2014). Therefore, the origins of sediments and the sedimentary processes likely differ across sedimentary environments (Fig. 8d).

https://doi.org/10.1017/qua.2017.43 Published online by Cambridge University Press

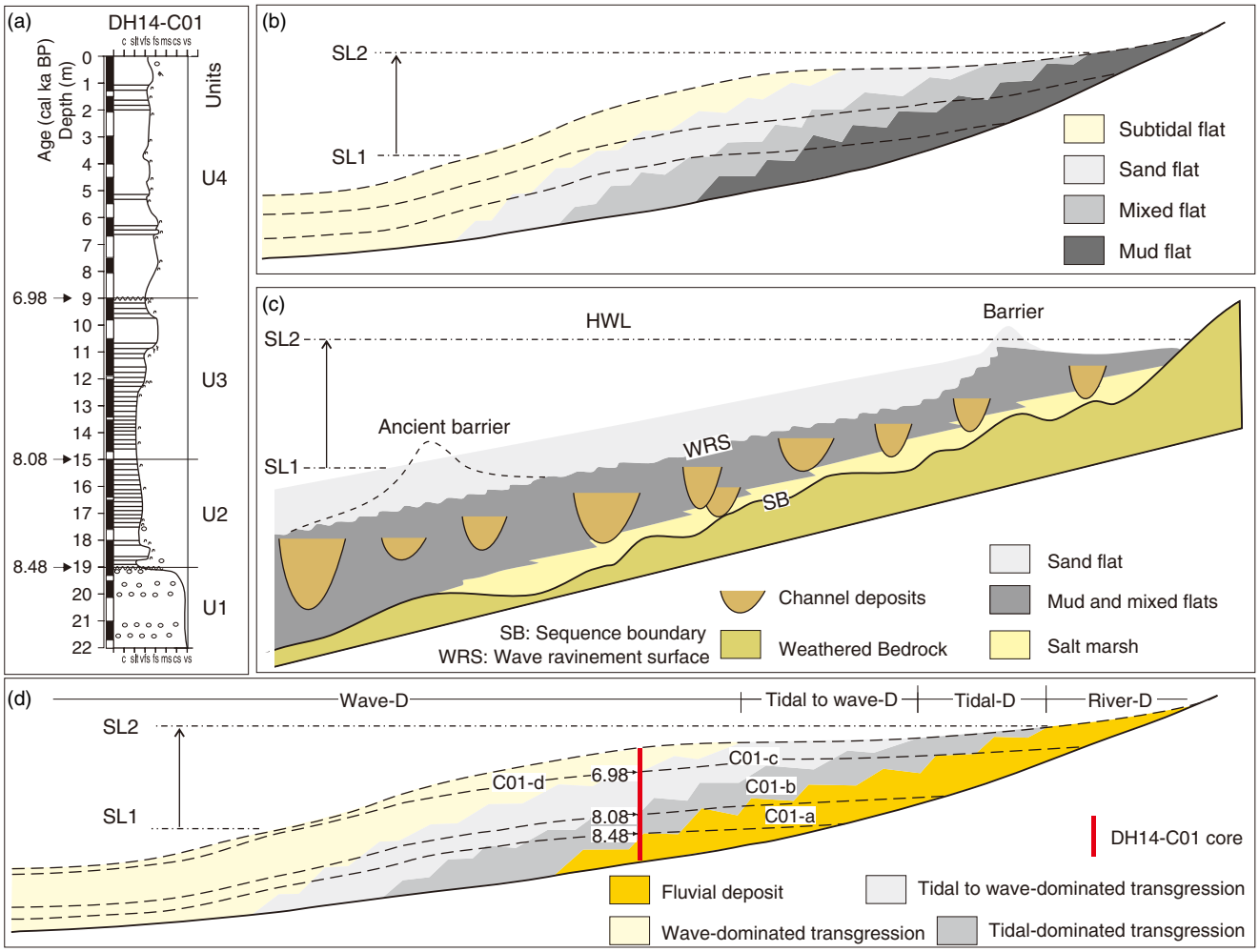

Figure 8. (color online) Sedimentary model of the Holocene. (a) Lithology of core 14DH-C01. (b) Sedimentary model of the tidal flat in Gomso Bay (Kim et al., 1999; Fan, 2012). (c) Sedimentary model of the area adjacent to Gomso Bay (Yang et al., 2006; Fan, 2012). (d) Holocene sedimentary model. SL, sea level; Wave-D, wave-dominated.

Fluvial deposition occurred during the early Holocene to 8.48 cal ka BP, and the sediment was clearly derived from the river drainage area. In the tide-dominated transgression period (8.48–8.08 cal ka BP), the sediments likely also primarily came from the river drainage area. However, during the transgression stage of tide- to wave-dominated deposition (8.08–6.98 cal ka BP), the transport of marine sediments to the study area by wave motion gradually increased. After 6.98 cal ka BP, wave-dominated processes controlled deposition, and the sediments were mainly derived from marine sands. The surface sediments of the East Yellow Sea are sands (Fan, 2012), and the grain size of surface sediments in Gomso Bay gradually coarsens and the slope gradient gradually steepens in the seaward direction (Lee et al., 1994; Yang et al., 2007).

Comparison with other large river mouth areas

Previous studies have described the paleoenvironmental changes in large river mouth areas, such as Mekong (Tamura et al., 2009), Red (Hori et al., 2004), and Changjiang Rivers (Hori et al., 2001a, 2001b; Wang et al., 2010; Song et al., 2013). These three areas share a similar Holocene sedimentary model (Hori et al., 2001a, 2001b, 2004; Tamura et al., 2009; Song et al., 2013; Feng et al., 2016), which may be divided into three stages (Fig. 9), as follows: retrogradation with a rapid rise in sea level during the early Holocene to 8.5 cal ka BP; progradation with decreasing sea level between 8.5 and 6.5 cal ka BP, bounded by a maximum flooding surface (Fig. 9); and progradation with a relatively stable sea level from 6.5 cal ka BP to the present.

A similar transgression occurred in the mouth of Gomso Bay from the early Holocene to 8.5 cal ka BP. In the study area, retrogradation occurred between 8.5 and 6.5 cal ka BP, with only a change from tide-dominated to wave-dominated tidal fill. After about 6.5 cal ka BP, the sedimentation processes widely differed between our study area and other large river areas.

The sedimentation process in a river mouth area is determined by sea level and sediment supply (Boyd et al., 1992,

https://doi.org/10.1017/qua.2017.43 Published online by Cambridge University Press

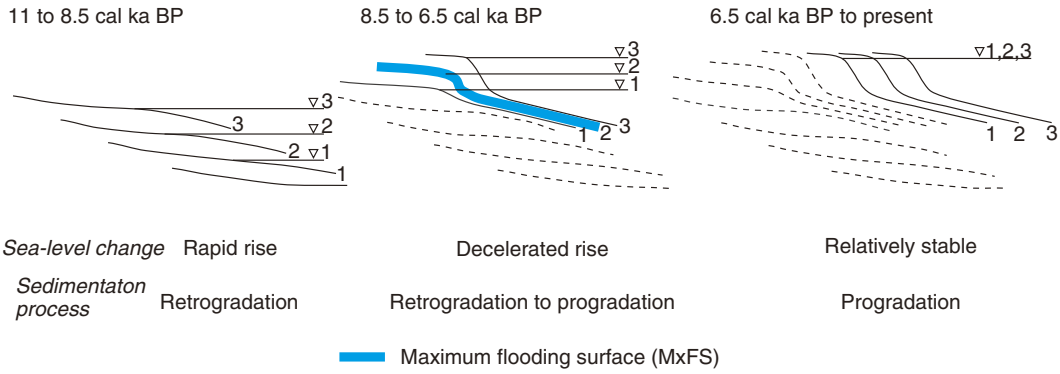

Figure 9. (color online) A general Holocene sedimentary model of large river mouth areas (e.g., Mekong [Tamura et al., 2009], Red [Hori et al., 2004], and Changjiang Rivers [Hori et al., 2001a]).

2006). Transgression occurs if the rate of sea-level rise is greater than the sedimentation rate, whereas regression occurs if the rate of sea-level rise is lower than the sedimentation rate. If the local factors are not considered, the sea-level changes in our study area during the Holocene are similar to those of other large river mouth areas. It is thus believed that the differences in the sedimentation processes led to differences in the sediment supply between our study area and other areas (Boyd et al., 1992, 2006).

CONCLUSION

We used high-resolution AMS ^{14}C dating, sediment-composition, grain-size, texture, and palynomorph analyses of core sediments sampled from the mouth of Gomso Bay to reconstruct the environmental history of the area during the Holocene.

The changes in the sedimentary environment in the study area during the Holocene were divided into four stages. River-dominated fluvial deposition occurred during the early Holocene to 8.48 cal ka BP, followed by a tide-dominated tidal channel fill transgression from 8.48 to 8.08 cal ka BP, a tide- to wave-dominated transgression from 8.08 to 6.98 cal ka BP, and a wave-dominated transgression from 6.98 ka BP to the present. Sedimentary evolution during the Holocene is closely tied to changes in sea level. The tidal channel fill transgression during mid-Holocene indicates a relatively high sedimentation rate in the study area.

Comparing our data with those from previous studies, we developed a sedimentary model for the Holocene in Gomso Bay and determined the provenances of the sediments. The changes in the sedimentary environment during the Holocene were determined by changes in sea level and the accompanying hydrodynamics. Transgressive deposition dominated, controlled by the different hydrodynamics of river-dominated, tide-dominated, tide- to wave-dominated, and wave-dominated processes during the different periods following changes in sea level. However, in other large river mouth areas, progradation dominated since the mid-Holocene. Hence, we conclude that the differences in the sedimentation processes have led to differences in the sediment supply between our study area and other large river mouth areas.

ACKNOWLEDGMENTS

This study was supported by a research grant from the Korean Ministry of Oceans and Fisheries (PJT200538) and the Basic Research Project (GP2017-013) grant of the Korea Institute of Geoscience and Mineral Resource funded by the Ministry of Science, ICT, and Future Planning, and funds from the Chinese Natural Science Foundation (Nos. 41271205 and 41401230). We thank Prof. Yoshiki Saito for providing suggestions and an English language editing service from Textcheck for improving the language of our manuscript. We greatly appreciate the assistance of editors Derek Booth and Peter Langdon, and thank two anonymous reviewers for their comments and suggestions that improved the manuscript.

SUPPLEMENTARY MATERIAL

To view supplementary material for this article, please visit https://doi.org/10.1017/qua.2017.43

REFERENCES

Academia Sinica. 1976. Sporae pteridophytorum sinicorum. [In Chinese.] Science Press, Beijing.

Academia Sinica. 1979. Angiosperm pollen flora of tropical and subtropical China. [In Chinese.] Science Press, Beijing.

Bak. 2015. Mid-Holocene sea-level fluctuation inferred from diatom analysis from sediments on the west coast of Korea. *Quaternary International* 384, 139–144.

Boyd, R., Dalrymple, R., Zaitlin, B., 1992. Classification of clastic coastal depositional environments. *Sedimentary Geology* 80, 139–150.

Boyd, R., Dalrymple, R., Zaitlin, B., 2006. Estuarine and incised-valley facies models. In: Posamentier, H.W., Walker, R. (Eds.), *Facies Models Revisited. SEPM Society for Sedimentary Geology*. Tulsa, pp. 180–181.

Blaauw, M., 2010. Methods and code for 'classical' age-modeling of radiocarbon sequences. *Quaternary Geochronology* 51, 512–518.

Blaauw, M., Christen, J., 2011. Flexible Paleoclimate age-depth models using an autoregressive Gamma process. *Bayesian Analysis* 6, 457–474.

Blaauw, M., Christen, J., 2013. Bacon Manual. http://chrono.qub.ac.uk/blaauw/.

Bronk Ramsey, C., Lee, S., 2013. Recent and planned developments of the program OxCal. *Radiocarbon* 55, 2–3.

Byeong-O, Jang, Yang, D., Kim, J., Choi, K., 2006. Postglacial vegetation history of the central western region of the Korean

Peninsula. [In Korean with English abstract.] *Journal of Ecology and Field Biology* 29, 573–580.
Chang, J.H., Choi, J. Y., 2001. Tidal-flat sequence controlled by Holocene sea-level rise in Gomso Bay, west coast of Korea. *Estuarine and Coastal Shelf Science* 52, 391–399.
Chang, J.H., Park, Y., Han, S., 1996. Late Quaternary stratigraphy and sea level change in the tidal flat of Gomso Bay, west coast of Korea. [In Korean with English abstract.] *Korean Society of Oceanography* 1, 59–72.
Chen, Z., Stanley, D., 1998. Sea-level rise in eastern China's Yangtze delta. *Journal of Coastal Research* 14, 360–366.
Chen, Z., Zong, Y., Wang, Z., Wang, H., Chen, J., 2008. Migration patterns of Neolithic settlements on the abandoned Yellow and Yangtze River deltas of China. *Quaternary Research* 70, 301–314.
Choi. 2011. Tidal rhythmites in a mixed-energy, macrotidal estuarine channel, Gomso Bay, west coast of Korea. *Marine Geology* 280, 105–115.
Choi, K., Hong, C., Kim, M., Oh, C., Jug, J., 2013. Morphologic evolution of macrotidal estuarine channels in Gomso Bay, west coast of Korea: implications for the architectural development of inclined heterolithic stratification. *Marine Geology* 346, 343–354.
Chough, S. K., Lee, H. J., Yoon, S. H., 2000. *Marine Geology of Korean Seas*. 2nd ed. Elsevier, Amsterdam.
Coleman, J.M., Wright, L.D., 1975. Modern river deltas: Variability of processes and sand bodies. In: Broussard, M.L. (Ed.), *Deltas, Models for Exploration*. Houston Geological Society, Houston, pp. 99–149.
Dalrymple, R., Zaitlin, B., Boyd, R., 1992. Estuarine facies models: Conceptual basis and stratigraphic implications. *Journal of Sedimentary Petrology* 62, 1130–1146.
Faegri, K., Iversen, J., 1989. *Textbook of pollen analysis*. In Faegri, K., Kaland, P.E., and Krzywinski, K., (Eds.), 4th ed. Wiley, New York.
Fan, D., 2012. Open-coast tidal flats. In: Davis, R. A., Jr., Dalrymple, R.W. (Eds.), *Principles of Tidal Sedimentology*. Springer, New York, pp. 187–229.
Feng, Z., Liu, B., Zhao, Y., Li, X., Dada, O., Jiang, L., Si, S., 2017. Structure, distribution, and evolution history of the Early Holocene erosional mud ridge system on the inner East China Shelf near the Yangtze River estuary. *Geomorphology* 283, 173–188.
Feng, Z., Liu, B., Zhao, Y., Li, X., Jiang, L., Si, S., 2016. Spatial and temporal variations and controlling factors of sediment accumulation in the Yangtze River estuary and its adjacent sea area in the Holocene, especially in the Early Holocene. *Continental Shelf Research* 125, 1–17.
Grimm, E. C., 1991. *TILIA.GRAPH* [computer software]. Illinois State Museum, Springfield, IL.
Grimm, E. C., 1992. *TILIA* [computer software]. Illinois State Museum, Springfield, IL.
Hori, K, Saito, Y, Zhao, Q, Cheng, X, Wang, P, Sato, Y, Li, C, 2001a. Sedimentary facies and Holocene progradation rates of the Changjiang (Yangtze) delta, China. *Geomorphology* 41, 233–248.
Hori, K., Saito, Y., Zhao, Q., Cheng, X., Wang, P., Sato, Y., Li, C., 2001b. Sedimentary facies of the tide-dominated paleo-Changjiang (Yangtze) estuary during the last transgression. *Marine Geology* 177, 331–351.
Hori, K., Saito, Y., Zhao, Q., Wang, P., 2002. Evolution of the coastal depositional systems of the Changjiang (Yangtze) River in response to late Pleistocene-Holocene sea-level changes. *Journal of Sedimentary Research* 72, 884–897.
Hori, K., Tanabe, S., Saito, Y., Haruyama, S., Nguyen, V., Kitamura, A., 2004. Delta initiation and Holocene sea-level change: Example from the Song Hong (Red River) delta, Vietnam. *Sedimentary Geology* 164, 237–249.
Intergovernment Panel on Climate Change (IPCC). 2014. Climate Change 2014: Synthesis Report. IPCC, Geneva, Switzerland.
Jun, C., Yi, S., Lee, S., 2010. Palynomorph implications of Holocene vegetation and environment in Pyeongtaek wetland, Korea. *Quaternary International* 227, 68–74.
Kang, J., Woo, H., Lee, Y., Son, Y., 2014. Seasonal sedimentary processes of the macrotidal flat in Gomso Bay, Korea. *Journal of Coastal Research* 70, 157–163.
Kim, Y. H., Lee, H. J., Chun, S. S., Han, S.J., Chough, S. K., 1999. Holocene transgressive stratigraphy of a macrotidal flat in the southeastern Yellow Sea: Gomso Bay, Korea. *Journal of Sedimentary Research* 69, 328–337.
Korean Meteorological Association (KMA). 1998. Annual climatological report. KMA, Seoul.
Korean Ocean Research and Development Institute (KORDI). 2007. Integrated preservation study on the marine environments in the Saemangeum area (1st year of 2nd phase, 2006). Annual Report 37907–18615. KORDI, Ansan, Korea.
Kong, G., Lee, C., 2005. Marine reservoir corrections (ΔR) for southern coastal waters of Korea. *The Sea, Journal of the Korean Society of Oceanography* 10, 124–128.
Li, Z., Saito, Y., Matsumoto, E., Wang, Y., Haruyama, S., Hori, K., Doanh, L., 2006. Palynomorph record of climate change during the last deglaciation from the Song Hong (Red River) delta, Vietnam. *Palaeogeography, Palaeoclimatology, Palaeoecology* 235, 406–430.
Lee, H., 2010. Preliminary results on suspended sediment transport by tidal currents in Gomso Bay, Korea. *Ocean Science Journal* 45, 187–195.
Lee, H., Chun, S., Chang, J., Han, S., 1994. Landward migration of isolated shelly sand ridge (Chenier) on the macrotidal flat of Gomso Bay, west coast of Korea: Control of storms and typhoons. *Journal of Sedimentary Research* 64, 886–893.
Lee, H., Chu, Y., Park, Y., 1999. Sedimentary processes of fine-grained material and the effect of seawall construction in the Daeho macrotidal flat nearshore area, northern west coast of Korea. *Marine Geology* 157, 171–184.
Munyikwa, K., Choi, J., Choi, K., Byun, J., Kim, J., Park, K., 2008. Coastal dune luminescence chronologies indicating a mid-Holocene highstand along the east coast of the Yellow Sea. *Journal of Coastal Research* 24, 92–103.
Nahm, W., Hong, S., 2014. Holocene environmental changes inferred from sedimentary records in the lower reach of the Yeongsan River, Korea. *The Holocene* 24, 1798–1809.
National Geography Information Institute (NGII). 1981. Basic research report on nearshore environments of Korea (Seokpo Area). Seoul, Korea.
National Oceanographic Research Institute (NORI). 2007. 2008 Tide Table (coast of Korea). Korean National Oceanographic Research Institute, Incheon, Korea.
Oh, H.-K., Rho, J.-H., 2013. Distribution characteristics of halophyte resources in a wetland protected area in the Gomso Bay. [In Korean with English abstract.] *The Journal of the Korean Institute of Forest Recreation* 17, 127–140.
Park, J., Yi, S., Oh, H., Xue, B., 2015. Holocene shoreline displacement on the Gungnam Plain, Buyeo, near the central west coast of South Korea inferred from diatom assemblages. *Quaternary International* 384, 129–138.

https://doi.org/10.1017/qua.2017.43 Published online by Cambridge University Press

Reimer, P., Bard, E., Bayliss, A., Beck, J., Blackwell, P., Ramsey, C., Buck, C., *et al*. 2013. IntCal13 and marine13 radiocarbon age calibration curves 0–50,000 year cal BP. *Radiocarbon* 55, 1869–1887.

Shin, H., Lim, D., Park, S., Heo, S., Kim, S., 2013. Distribution of dinoflagellate cysts in Yellow Sea sediments. *Acta Oceanologica Sinica* 32, 91–98.

Shin, H., Matsuoka, K., Yoon, Y., Kim, Y., 2010. Response of dinoflagellate cyst assemblages to salinity changes in Yeojia Bay, Korea. *Marine Micropaleontology* 77, 15–24.

Shin, H., Yoon, Y., Matsuoka, K., 2007. Modern dinoflagellate cyst distribution off the eastern part of Geoje Island, Korea. *Ocean Science Journal* 42, 31–39.

Song, B., Li, Z., Saito, Y., Okuno, J., Li, Z., Lu, A., Hua, D., Li, J., Li, Y., Nakashima, R., 2013. Initiation of the Changjiang (Yangtze) delta and its response to the mid-Holocene sea-level change. *Palaeogeography, Palaeoclimatology, Palaeoecology* 388, 81–97.

Stanley, D. J., Warne, A.G., 1994. Worldwide initiation of Holocene marine deltas by deceleration of sea-level rise. *Science* 265, 228–231.

Tamura, T., Saito, Y., Sieng, S., Ben, B., Kong, M., Choup, S., Tsukawaki, S., 2007. Depositional facies and radiocarbon ages of a drill core from the Mekong River lowland near Phnom Penh, Cambodia: evidence for tidal sedimentation at the time of Holocene maximum flooding. *Journal of Asian Earth Sciences* 29, 585–592.

Tamura, T., Saito, Y., Sieng, S., Ben, B., Kong, M., Sim, I., Choup, S., Akiba, F., 2009. Initiation of the Mekong River delta at 8 ka: Evidence from the sedimentary succession in the Cambodian lowland. *Quaternary Science Reviews* 28, 327–344.

Wang, Z., Li, M., Zhang, R., Zhuang, C., Liu, Y., Saito, Y., Xie, J., Zhao, B., 2011. Impacts of human activity on the late-Holocene development of the subaqueous Yangtze delta, China, as shown by magnetic properties and sediment accumulation rates. *The Holocene* 21, 393–407.

Wang, Z., Xu, H., Zhan, Q., Saito, Y., He, Z., Xie, J., Li, X., Dong, Y., 2010. Lithological and palynomorph evidence of late Quaternary depositional environments in the subaqueous Yangtze delta, China. *Quaternary Research* 73, 550–562.

Wang, Z., Zhan, Q., Long, H., Saito, Y., Gao, X., Wu, X., Li, L., Zhao, Y., 2013. Early to mid-Holocene rapid sea-level rise and coastal response on the southern Yangtze delta plain, China. *Journal of Quaternary Science* 28, 659–672.

Wells, J., Adams, C. Jr., Park, Y., Frankenberg, E., 1990. Morphology, sedimentology and tidal channel processes on high-tide-range mudflats, west coast of South Korea. *Marine Geology* 95, 111–130.

Yang, B., Dalrymple, R., Chun, S., Lee, H., 2006. Transgressive sedimentation and stratigraphic evolution of a wave-dominated macrotidal coast, western Korea. *Marine Geology* 235, 35–48.

Yang, B., Dalrymple, R., Gingras, M., Chun, S., Lee, H., 2007. Up-estuary variation of sedimentary facies and ichnocoenoses in an open-mouthed, macrotidal, mixed-energy estuary, Gomso Bay, Korea. *Journal of Sedimentary Research* 77, 757–771.

Yi, S., Saito, Y., Oshima, H., Zhou, Y., Wei, H., 2003. Holocene environmental history inferred from pollen assemblages in the Huangehe (Yellow River) delta, China: climate change and human impacts. *Quaternary Science Reviews* 22, 609–628.

Zonneveld, K., Marret, F., Versteegh, G., Bogus, K., Bonnet, S., Bouimetarhan, I., Crouch, E., *et al*. 2013. Atlas of modern dinoflagellate cyst distribution based on 2405 data points. *Review of Palaeobotany and Palynomorphs* 191, 1–197.

Zong, Y., 2004. Mid-Holocene sea-level highstand along the Southeast Coast of China. *Quaternary Research* 117, 55–67.

https://doi.org/10.1017/qua.2017.43 Published online by Cambridge University Press